Available online at www.sciencedirect.com
SCIENCE DIRECT®

Chemical Physics Letters 412 (2005) 23–28

CHEMICAL PHYSICS LETTERS

www.elsevier.com/locate/cplett

Global minima and energetics of $Li^+(H_2O)_n$ and $Ca^{2+}(H_2O)_n$ clusters for $n \leqslant 20$

Briesta S. González [a], Javier Hernández-Rojas [a,*], David J. Wales [b]

[a] Departamento de Física Fundamental II, Universidad de La Laguna, 38205 Tenerife, Spain
[b] University Chemical Laboratories, Lensfield Road, Cambridge CB2 1EW, United Kingdom

Received 26 May 2005; in final form 23 June 2005
Available online 14 July 2005

Abstract

We present candidate structures for the global potential energy minima of $X(H_2O)_n$ ($X = Li^+$, Ca^{2+}) clusters with $n \leqslant 20$. The TIP4P rigid body water–water potential is employed, together with cation–water interactions that are represented as a sum of Coulomb and Lennard–Jones terms. We find that in the Li^+ global minima the cation tends to be located on the cluster surface with a preferred coordination number of four water molecules in tetrahedral positions. In contrast, for Ca^{2+} clusters the cation occupies an interior site surrounded by eight water molecules in a square anti-prismatic arrangement.

---

1. Introduction

For several decades, the study of ions in aqueous solution has been an area of intensive scientific investigation. One of the fundamental aspects that attracts considerable research interest is the determination of the coordination number of the ion in the first solvation shell. This subject has been studied both experimentally [1] and theoretically [2]. The evolution of the coordination environment with the number of water molecules in an ion–water cluster is also of interest. Small systems are likely to exhibit different properties from bulk, because most atoms are in a surface environment. However, for large enough clusters the bulk limit should be recovered.

Global optimisation of pure water clusters [3–6], and of protonated water clusters [7,8] using rigid body empirical potentials has proved to be relatively difficult compared to atomic clusters with a comparable number of degrees of freedom. The difficulty is basically due to the coupling between the angular and centre-of mass degrees of freedom, which gives rise to a hierarchical potential energy landscape [9,10]. Our aim in the present work is to extend our previous global optimisation studies to cation–water clusters. Using a simple potential energy surface (PES) based on Lennard–Jones and Coulomb terms, and the basin-hopping global optimisation approach, we have determined likely global potential energy minima for Li^+ and Ca^{2+} cation–water clusters. For the resulting structures we report the cation coordination number and analyse how the different contributions to the potential energy change with the number of water molecules. We also consider the hydrogen-bonding pattern within the water network in some detail.

This Letter is organised as follows. In the following section, we describe the PES and the global optimisation method employed. In Section 3, we present and discuss the results. Finally, Section 4 summarises our conclusions.

2. Methods

The closed-shell electronic structure of the water molecule and the chosen ions makes semi-empirical methods

---

[*] Corresponding author.
E-mail addresses: jhrojas@ull.es (J. Hernández-Rojas), dw34@cam.ac.uk (D.J. Wales).

0009-2614/$ - see front matter © 2005 Elsevier B.V. All rights reserved.
doi:10.1016/j.cplett.2005.06.090

particularly appropriate for modelling the PES. In describing the interactions of the corresponding clusters have adopted relatively simple functional forms without polarisation terms to reduce the computational expense, as discussed below. We separate the total energy as

$$U_{\text{tot}} = U_{\text{water–water}} + U_{\text{ion–water}}, \tag{1}$$

where the first term corresponds to the water–water interaction and is represented by the well-known TIP4P potential [11]. In this model, the water molecules are treated as rigid bodies with a hydrogen–oxygen distance of 0.9572 Å and a hydrogen–oxygen–hydrogen (HOH) angle of 104.52°. The interaction between water molecules is described by a pairwise potential of Lennard–Jones and Coulomb terms, given by the expression

$$U_{\text{water–water}} = \sum_{i<j}^{n} \left[4\epsilon_{\text{O}} \left\{ \left(\frac{\sigma_{\text{O}}}{r_{\text{O}_i\text{O}_j}} \right)^{12} - \left(\frac{\sigma_{\text{O}}}{r_{\text{O}_i\text{O}_j}} \right)^{6} \right\} + A \sum_{k_i=1}^{3} \sum_{k_j=1}^{3} \frac{q_{k_i} q_{k_j} e^2}{r_{k_i k_j}} \right],$$

where the sum over i and j refers to separate water molecules, and the sum over k_i and k_j refers to the charge sites on molecules i and j. The Lennard–Jones term is applied between oxygen atoms, and the parameters are $\epsilon_{\text{O}} = 0.648\ \text{kJ mol}^{-1}$ and $\sigma_{\text{O}} = 3.153$ Å. We measure the distances in Å so that the energy is in kJ mol^{-1}. Two of the water point charges are located on the hydrogen atoms, with $q_{\text{H}} = 0.52$, and the third charge is $q_{\text{M}} = -1.04$, located at a distance of 0.15 Å from the oxygen atom on a line bisecting the HOH angle. A is a unit conversion factor whose numerical value is $1389.35\ \text{kJ mol}^{-1}$ Å when e is the magnitude of the charge on an electron in coulomb, so that the q parameters are effectively multiples of this elementary charge. The number of water molecules is denoted as n.

The second term of Eq. (1) represents the interaction between the ion and the water molecules. It is also represented as a sum of Lennard–Jones and Coulomb potentials and is given by

$$U_{\text{ion–water}} = \sum_{i=1}^{n} \left[4\epsilon_{\text{XO}} \left\{ \left(\frac{\sigma_{\text{XO}}}{r_{\text{XO}_i}} \right)^{12} - \left(\frac{\sigma_{\text{XO}}}{r_{\text{XO}_i}} \right)^{6} \right\} + A \sum_{k_i=1}^{3} \frac{q_X q_{k_i} e^2}{r_{Xk_i}} \right], \tag{2}$$

where the parameters used here, ϵ_{XO}, σ_{XO}, and q_{X}, are listed in Table 1. These parameters are taken from the literature [12].

The simplicity of this potential energy function, and the good qualitative agreement with other more complicated representations [13], have motivated a number of other recent studies [2,12,14]. Furthermore, polarisation effects have been shown to be small or negligible in cation–water clusters [14]. In contrast, including polarisation terms [15–17] seems to be important in order to obtain an accurate description of the structure in anion–water clusters [18,19]. However, the non-polarisable model is expected to give reasonably good energies and structures for the cation–water clusters considered in the present work. In fact, we will show in the next section that with this simple model we obtain the same lowest energy structures as calculated with ab initio methods [20,21] for $\text{Li}^+(\text{H}_2\text{O})_n$ ($n = 1$–6), as well as good agreement with experimental results for the coordination of Ca^{2+} in aqueous solution [22,23].

Table 1
Parameters employed for the ion–water potential

X	ϵ_{XO} (kJ/mol)	σ_{XO} (Å)	q_{X} (e)
Li^+	0.669	2.330	+1
Ca^{2+}	0.521	3.024	+2

The global potential energy minima were located using the basin-hopping scheme [24] (a Monte-Carlo plus minimisation approach [25]). This method has been used successfully in both neutral [24] and charged clusters [26–29], along with many other applications [10]. Each water molecule, treated as a rigid body, has six degrees of freedom represented in terms of three centre of mass coordinates, (X, Y, Z), and three components of a vector $\vec{k} = (n, l, m)$, which define a rotation axis through the centre of mass of a reference structure [30]. The magnitude of the rotation is $\alpha = \sqrt{n^2 + l^2 + m^2}$. This angle–axis representation has been recently introduced into the public domain global optimisation program GMIN to provide a a general framework for rigid body isotropic site–site potentials.

As in previous studies [3,7], we have determined suitable parameters for the basin-hopping calculations using a number of runs for one particular cluster, which was chosen as $\text{Li}^+(\text{H}_2\text{O})_{12}$ in the present work. Basin-hopping runs consisting of 30 000 steps (minimisations) were started from independent random geometries at different temperatures and with different fixed acceptance ratios [24]. Separate blocks of 100 centre of mass and 200 angular moves were performed. The same lowest-energy minimum was found in all simulations. The results described in the following section were obtained at a constant temperature of $k_BT = 2\ \text{kJ mol}^{-1}$ and an acceptance ratio of 0.1, which produced the shortest first encounter time for the global minimum of $\text{Li}^+(\text{H}_2\text{O})_{12}$. A total of 20 runs of 30 000 basin-hopping steps each were performed for $n \leqslant 16$ and 5 runs of 50 000 steps each for each size $n \geqslant 17$. In the larger clusters the same lowest energy minimum was not found in every run, and it is possible that the putative global minima for $n \geqslant 17$ may be improved in the future. Nevertheless, the structures that we have located are likely to be representative in terms of features such as the ion coordination number.

3. Results

In this section, we present the likely candidates for the global potential energy minima of $Li^+(H_2O)_n$ and $Ca^{2+}(H_2O)_n$. These structures will be made available for download from the Cambridge Cluster Database [31]. For the $X(H_2O)_n$ complexes, association energies [27,28] are defined for the process

$$n(H_2O) + X = X(H_2O)_n; \quad \Delta E_a. \tag{3}$$

We also define the X ion binding energy [27,28] as the difference between the association energy of the complex and that of the $(H_2O)_n$ cluster, i.e.,

$$(H_2O)_n + X = X(H_2O)_n; \quad \Delta E_b. \tag{4}$$

3.1. Li^+–water clusters

In Fig. 1a, we plot the association and binding energies as a function of the number of water molecules, n. Both of these energies tend to asymptotic values as n increases. The initial sharp decrease shown by the binding energies in this figure is related to the formation of the first ion coordination shell [27,28]. The Li^+ cation has a lower coordination number, with the ion surrounded by four water molecules in tetrahedral positions in most of the global minima, and a local site symmetry defined by the S_4 point group. The average distance between the ion and the oxygen atoms is around 1.97 Å. This result is in very good agreement with recent ab initio simulations [32] and experimental data [33]. The corresponding 'microsolvation' structure is plotted in Fig. 2.

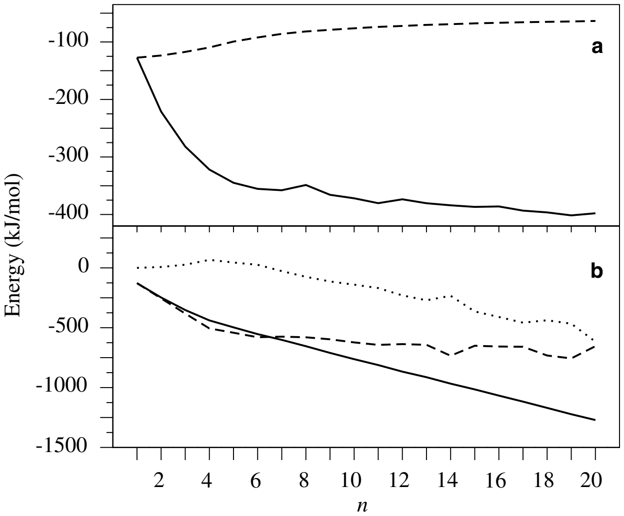

Fig. 1. Predicted energetics for $Li^+(H_2O)_n$ global minima. (a) Association energies per water molecule $\Delta E_a/n$ (dashed line) and binding energies ΔE_b (solid line). (b) Total energies U_{tot} (solid line), water–water energies $U_{water–water}$ (dotted line) and ion–water energies $U_{ion–water}$ (dashed line).

Once the first ion coordination shell is completed hydrogen-bonds between water molecules start to appear. In general, we find that the number of hydrogen-bonds increases with n, except for $n = 14$, which has the same number as $n = 13$. Furthermore, for $n = 14$, $n = 18$, and $n = 19$ the ion favours a different environment involving six, five, and five water molecules, respectively. In these global minima, the mean distance between the ion and the oxygen atom in the water molecule increases to 2.1 Å.

In order to understand this behaviour better Fig. 1b indicates the different contributions to the total potential energy. U_{tot}, $U_{water–water}$, and $U_{ion–water}$ are plotted against the number of water molecules, n. When the Li^+ cation is surrounded by four water molecules $U_{water–water}$ reaches a maximum value (positive), which is related to the lack of hydrogen-bonds in the structure. For $n \geqslant 5$ this contribution decreases almost linearly, except for $n = 14$, $n = 18$, and $n = 19$, where peaks arise because a modification of the coordination number occurs. The $U_{ion–water}$ term also reaches a limiting value around $n = 4$, when the preferred environment is formed.

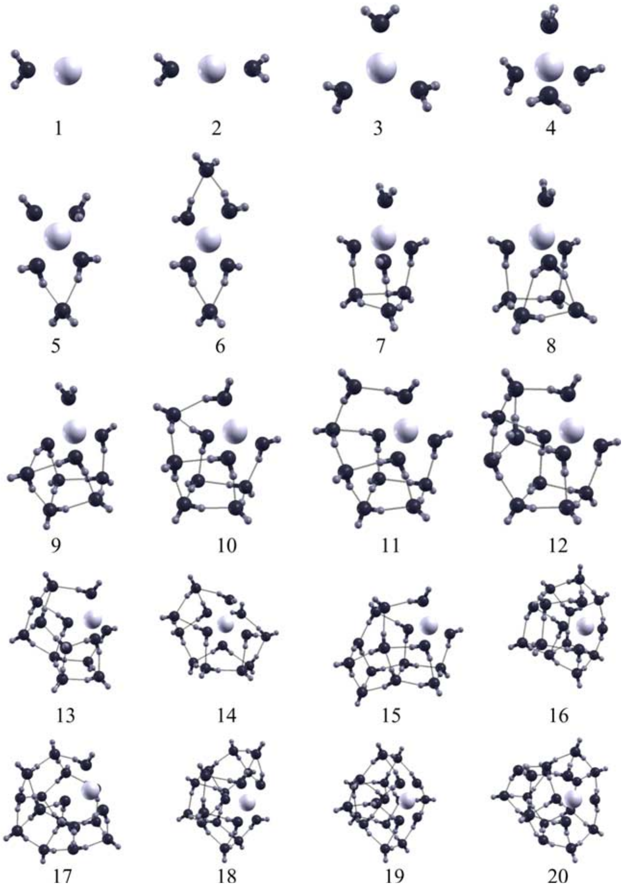

Fig. 2. Global minimum structures for $Li^+(H_2O)_n$ ($n = 1$–20) clusters labelled according to the number of water molecules. All the figures involving cluster structures were prepared using the program XCRYSDEN [34].

All global minimum structures located for this system are shown in Fig. 2. The first six cation–water clusters are in good agreement with recent ab initio calculations [20,21]. Furthermore, the ion preferentially occupies a site in the cluster surface, in agreement with molecular dynamics simulations at finite temperature [12].

3.2. Ca^{2+}–water clusters

The larger σ_{XO} and q_X values for Ca^{2+} produce a different coordination environment in the corresponding water clusters. In Fig. 3a, we plot $\Delta E_a/n$ and ΔE_b as a function of the number of water molecules. As n increases, both energies tend to asymptotic values. As for the Li^+ clusters, the initial sharp decrease of the binding energies is related to the formation of the first coordination shell. In this case, the Ca^{2+} cation prefers a higher coordination number, defined by eight water molecules in a square anti-prismatic arrangement. The site symmetry in this case is defined by the point group S_8, as shown in Fig. 4. Here, the average distance between the ion and the surrounding oxygen atoms is around 2.51 Å. This value is in good agreement with recent experimental data for Ca^{2+} in aqueous solution [22,23], and with classical molecular dynamics simulations [35] at finite temperature. In this first ion coordination shell hydrogen-bonds are not formed, and the water–water interaction reaches an unfavourable maximum value at $n = 8$, whilst the ion–water interaction decreases slowly with n (Fig. 3b). For $n \geqslant 9$ hydrogen-bonds start to appear, and we generally observe two per water molecule for $n \geqslant 12$. For Ca^{2+} the cation prefers to be located inside the cluster, in agreement with molecular dynamics simulations [12]. All the global minima are illustrated in Fig. 4.

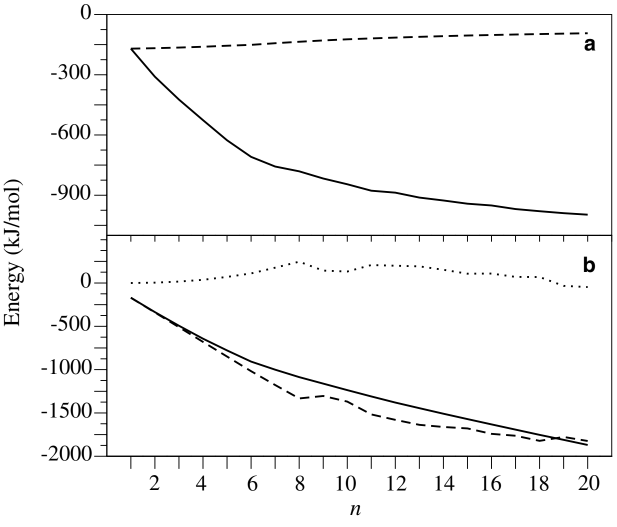

Fig. 3. Predicted energetics for $Ca^{2+}(H_2O)_n$ global minima. (a) Association energies per water molecule $\Delta E_a/n$ (dashed line) and binding energies ΔE_b (solid line). (b) Total energies U_{tot} (solid line), water–water energies $U_{water-water}$ (dotted line) and ion–water energies $U_{ion-water}$ (dashed line).

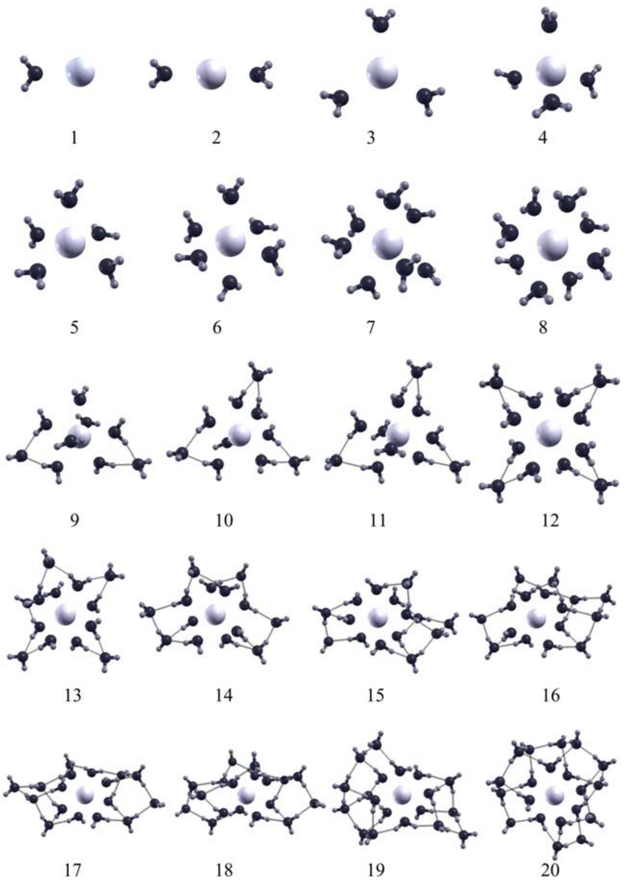

Fig. 4. Global minimum structures for $Ca^{2+}(H_2O)_n$ ($n = 1$–20) clusters labelled according to the number of water molecules.

4. Conclusions

Using a basin-hopping global optimisation scheme [24,25], we have located the likely global minima for $Li^+(H_2O)_n$ and $Ca^{2+}(H_2O)_n$ clusters with $n \leqslant 20$. From a simple potential energy function, based on the rigid non-polarisable TIP4P model, we find that the smallest Li^+ cation prefers to occupy a position on the water cluster surface surrounded by four water molecules in tetrahedral sites for the first coordination shell. These results are in good agreement with empirical [12] and ab initio simulations [32], and also with experimental data [33].

On the other hand, we find that the larger Ca^{2+} cation prefers a first coordination shell of eight water molecules in a square anti-prismatic arrangement, in good agreement with experimental data [22,23]. The increase of the cation size and charge make an internal position more favourable [12]. For $n \geqslant 12$, the number of hydrogen-bonds formed per water molecule is two.

The good agreement between our results and other more sophisticated techniques, as well as experimental data, supports the use of the simple potential energy used here for cation–water clusters. However, we also note that the global free energy minimum is likely to change from the global potential energy minimum at higher temperature.

Neither $Li^+(H_2O)_{20}$ nor $Ca^{2+}(H_2O)_{20}$ involve clathrate structures with the cation at the centre of a dodecahedron of water molecules. Similar behaviour has been reported for Na^+, while 'clathrate-like' cage structures were found for K^+ and Cs^+ in distorted dodecahedra [2]. These differences are clearly due to the energetic balance involved in solvating the cation and disrupting the hydrogen bonding network between the water molecules. Since we focus upon the global potential energy minimum entropy effects are not relevant, which simplifies the situation somewhat.

Clathrate-like structures appear to be less favourable for the three cations with the highest charge densities. It is these ions that would be able to form the strongest electrostatic interactions with water oxygen atoms, and these specific interactions will make a significant contribution to the total binding energy of the cluster compared to the water–water interactions in small systems. The number of strong cation–water contacts that can be formed for Li^+ and Ca^{2+} also depends upon their size, since the surrounding water molecules must avoid unfavourable steric clashes. The solvent molecules in the first coordination shell cannot form hydrogen bonds amongst themselves without introducing unfavourable electrostatic interactions with the cation, and hence the situation is reminiscent of the usual radius ratio rules for packing of inorganic solids.

Clathrate-type structures probably serve to maximise the favourable water–water interactions, whilst maintaining a reasonable electrostatic environment for the centre cation. However, for ions like Li^+ and Ca^{2+} it appears to be the particularly strong cation–water energetics that are optimised, at the expense of the water–water contribution. To check this interpretation, we placed each ion in the middle of the lowest TIP4P $(H_2O)_{20}$ dodecahedron and minimised the energy. We then compared the water–water and ion–water contributions to the potential energy in these local minima with the corresponding quantities in the true global minima. For Li^+ both contributions to the total energy are more favourable in the global minimum (by 5.8% and 2.6% for the water–water and water–ion terms, respectively). For Ca^{2+} the water–water contribution is actually less favourable in the true global minimum, but the water–ion term more than compensates for the lost water–water interactions. For this doubly charged ion the water–water contribution is less than 10% of the total potential energy for both the local minima, and hence we expect the structure of the global potential energy minimum to be primarily determined by optimal packing around the ion. The water–water and water–ion terms are comparable in the $Li^+(H_2O)_{20}$ clusters, and hence it seems likely that clathrate structures will only become competitive when the water–ion contribution decreases further, or the ions become larger, as for K^+ and Cs^+.

Acknowledgements

One of us (B.S.G.) gratefully acknowledges an FPU grant from the Spanish Ministry of Education and Science. Prof. J. Bretón and Prof. J.M. Gomez Llorente are acknowledged for helpful discussions. J.H.-R. gratefully acknowledges the support of the 'Ministerio de Ciencia y Tecnología' and 'FEDER fund (EU)' under Contract No. BFM2001-3343.

References

[1] U. Buck, F. Huisken, Chem. Rev. 100 (2000) 3863.
[2] F. Schulz, B. Hartke, Chem. Phys. Chem. 3 (2002) 98, and reference therein.
[3] D.J. Wales, M.P. Hodges, Chem. Phys. Lett. 286 (1998) 65.
[4] B. Hartke, Z. Phys. Chem. 214 (2000) 1251.
[5] H. Kabrede, R. Hentschke, J. Phys. Chem. B 107 (2003) 3914.
[6] J.K. Kazimirski, V. Buch, J. Phys. Chem. A 107 (2003) 9762.
[7] M.P. Hodges, D.J. Wales, Chem. Phys. Lett. 324 (2000) 279.
[8] T. James, D.J. Wales, J. Chem. Phys. 12 (2005) 134306.
[9] D.J. Wales, M.A. Miller, T.R. Walsh, Nature 394 (1998) 758.
[10] D.J. Wales, Energy Landscapes, Cambridge University Press, Cambridge, 2003.
[11] W.L. Jorgensen, J. Chem. Phys. 77 (1982) 4156.
[12] A.V. Egorov, E.N. Brodskaya, A. Laaksonen, J. Chem. Phys. 118 (2003) 6380.
[13] G.H. Peslherbe, B.M. Ladanyi, J.T. Hynes, J. Phys. Chem. A 104 (2000) 4533, and reference therein.
[14] O. Borodin, R.L. Bell, Y. Li, D. Bedrov, G.D. Smith, Chem. Phys. Lett. 336 (2001) 292.
[15] L.X. Dang, T.-M. Chang, J. Chem. Phys. 106 (1997) 8149, and reference therein.
[16] D.H. Herce, L. Perera, T.A. Darden, C. Sagui, J. Chem. Phys. 122 (2005) 024513, and reference therein.
[17] C.J. Burnham, J. Li, S.S. Xantheas, M. Leslie, J. Chem. Phys. 110 (1999) 4566.
[18] D.J. Tobias, P. Jungwirth, M. Parrinello, J. Chem. Phys. 114 (2001) 7036.
[19] S. Yoo, Y.A. Lei, X.C. Zeng, J. Chem. Phys. 119 (2003) 6083.
[20] H.M. Lee, P. Tarakeshwar, J. Park, M.R. Kolaski, Y.J. Yoon, H.-B. Yi, W.Y. Kim, K.S. Kim, J. Phys. Chem. A 108 (2004) 2949.
[21] I.B. Muller, L.S. Cederbaum, F. Tarantelli, J. Phys. Chem. A 108 (2004) 5831.
[22] P. D'Angelo, P.-E. Petit, N.V. Pavel, J. Phys. Chem. B 108 (2004) 11857.
[23] T. Megyes, T. Grósz, T. Radnai, I. Bakó, G. Pálinkás, J. Phys. Chem. A 108 (2004) 7261.
[24] D.J. Wales, J.P.K. Doye, J. Phys. Chem. A 101 (1997) 5111.
[25] Z. Li, H.A. Scheraga, J. Mol. Struct. 179 (1988) 333.
[26] J. Hernández-Rojas, D.J. Wales, J. Chem. Phys. 119 (2003) 7800.

[27] J. Hernández-Rojas, J. Bretón, J.M. Gomez Llorente, D.J. Wales, J. Chem. Phys. 121 (2004) 12315.

[28] J. Hernández-Rojas, J. Bretón, J.M. Gomez Llorente, D.J. Wales, Chem. Phys. Lett. 410 (2005) 404.

[29] J.P.K. Doye, D.J. Wales, Phys. Rev. B 59 (1999) 2292.

[30] D.J. Wales, Phil. Trans. Roy. Soc. A 363 (2005) 357.

[31] D.J. Wales, J.P.K. Doye, A. Dullweber, M.P. Hodges, F.Y. Naumkin, F. Calvo, J. Hernández-Rojas, T.F. Middleton, The Cambridge Cluster Database. Available from: <http://www-wales.ch.cam.ac.uk/CCD.html>.

[32] A.P. Lyubartsev, K. Laasonen, A. Laaksonen, J. Chem. Phys. 114 (2001) 3120.

[33] I. Howel, G.W. Neilson, J. Phys.: Condens. Matter 8 (1996) 4455.

[34] A. Kokalj, J. Mol. Graph. Model. 17 (1999) 176.

[35] S.G. Kalko, G. Sesé, J.A. Padro, J. Chem. Phys. 104 (1996) 9578.